Inverse Problems, Design and Optimization Symposium
Rio de Janeiro, Brazil, 2004

CONSTRAINED OPTIMIZATION OF AERODYNAMIC SHAPES VIA MINIMIZATION OF TOTAL DRAG

Sergey Peigin
Israel Aircraft Industries
Ben-Gurion Airport, 70100
speigin@iai.co.il

Boris Epstein
The Academic College of Tel-Aviv Yaffo
Computer Sciences Department
epstein@mta.ac.il

ABSTRACT

In this work a robust and efficient approach to the multipoint constrained design is developed and applied to the optimization of aerodynamic wings. The approach employs Genetic Algorithms (GAs) as an optimization tool in combination with a Reduced-Order Models (ROM) method based on linked local data bases obtained by full Navier-Stokes computations. The method was implemented in the computer code OPTIMAS (OPTI-Mization of Aerodynamic Shapes). The code was applied to the problem of multipoint 2D and 3D aerodynamic wing optimization. It was demonstrated that the optimization tool allows to find optima located exactly on the constraints boundary. The method retains high robustness of conventional GAs while keeping CFD computational volume to an acceptable level.

INTRODUCTION

The main objective of the present research is to create a powerful tool for aerodynamic design, which reduces the overall cost of aircraft design and analysis.

The requirements for the computational tool which will be capable to solve the above problem are rather high.

First, the problem of global geometrical representation of 3D aerodynamic shapes still remains open. Second, the construction of a reliable CFD solver suitable for optimization in terms of accuracy and robustness is a complicated task by itself. Third, the optimization requires the use of high-dimension search spaces which makes the optimal search highly non-trivial, especially in the presence of non-linear constraints. Finally, due to huge overall computational volume needed for optimization, additional requirements should be imposed on the computational efficiency of the whole method.

The full Navier-Stokes code NES [1-2] satisfies the requirements of high accuracy and robustness. In order to satisfy the requirement of fast computational feedback, we suggest to scan the optimization search space by using the Reduced-Order Models (ROM) approach [3] in the form of Local Approximation Method (LAM) based on local data bases obtained by full Navier-Stokes computations.

The presence of constraints significantly decreases the robustness and the computational efficiency of classical optimization methods [4]. The reason for this lies in the fact that the calculation of derivatives of the objective function in the vicinity of the constraints boundary is an ill-posed problem which can not be resolved by conventional methods. The situation is especially troublesome in the case of constraints imposed on aerodynamic characteristics (such as aerodynamic moments). In this case the question regarding feasibility of a current geometry can be answered only "a posteriori", that is only through a full CFD run.

In order to create a robust and computationally efficient optimization tool, Genetic Algorithms (GAs) were employed. A specific feature of the new approach consists in changing the conventional search strategy. The proposed algorithm employs search paths which pass via both feasible and infeasible points (contrary to the traditional approach where only feasible points may be included in a path).

PROBLEM FORMULATION

In the case of the single point optimization problem, the objective is to minimize the cost function (total drag coefficient C_D of a wing) subject to the following classes of constraints:

1) Aerodynamic constraints such as prescribed constant total lift coefficient C_L^* and maximum allowed pitching moment C_M^*.

2) Geometrical constraints on the shape of the wing surface in terms of properties of sectional airfoils - relative thickness $(t/c)_i$, relative radius of leading edge $(R/c)_i$, trailing edge angle θ_i, where $i = 1,..., N_{ws}$ (N_{ws} - the number of sectional airfolis), and $(t/c)_i^*$, θ_i^*, $(R/c)_i^*$, C_L^* and C_M^* are prescribed parameters of the problem.

The point design wing must be analyzed over a range of Mach numbers and lift coefficients to ensure the adequacy of the off-design performance. To reach this goal the multipoint optimization is needed where the objective function is a weighted combination of single point cost functions.

As a gas-dynamic model for calculating C_D, C_L and C_M values, the full Navier-Stokes equations are used. Numerical solution of the full Navier-Stokes equations is based on a multiblock code NES [1-2].

OPTIMIZATION ALGORITHM

As a basic algorithm, a variant of the floating-point GA is used [4]. Unfortunately, in their basic form, GAs are not capable of handling constraint functions limiting the set of feasible solutions. To resolve this, a new approach is suggested which can be basically outlined as follows:

1) Change of the conventional search strategy by employing search paths which pass through both feasible and infeasible points (instead of the traditional approach where only feasible points may be included in a path).

2) To implement the new strategy, it is suggested to extend the search space. This requires the evaluation (in terms of fitness) of the points, which do not satisfy the constraints imposed by the optimization problem. A needed extension of an objective function may be implemented by means of GAs due to their basic property: contrary to classical optimization methods, GAs are not confined to only smooth extensions.

This extension should only satisfy the condition that follows immediately from the main idea to increase a diversity of current population: in infeasible regions, the objective function should be defined in such a way that it keeps in the current population a certain number of infeasible individuals, which are located rather close to the constraint boundary. In such a case we can expect, with a rather high probability, that the crossover between feasible and infeasible individuals will produce high-fitness children.

In fact, this allows to find an optimal point located exactly on the constraints boundary. Contrary to the conventional penalty function method, the suggested approach does not modify the value of objective function in any feasible point. In this regard, the method implements a zero-penalty approach.

In this work it is assumed that:

1) For geometry description the absolute Cartesian coordinate system (x, y, z) is used.

2) Wing planform is fixed.

3) Wing surface is generated by linear interpolation (in the span direction) between sectional 2D airfoils.

4) The number of sectional airfoils N_{ws} is fixed.

5) Shape of sectional airfoils is determined by Bezier Splines.

Roughly speaking, each CFD run requires a different geometry and, therefore, the construction of a new computational grid, which is very time-consuming. In order to overcome this obstacle and to maintain the continuity of optimization stream, we made use of topological similarity of geometrical configurations (involved in the optimization process), and the grids are constructed by means of a fast automatic transformation of the initial grid which corresponds to the starting basic geometry.

One of the main weaknesses of GAs lies in their poor computational efficiency. In order to overcome this, we introduce an intermediate "computational agent" - a computational tool which, on the one hand, is based on a very limited number of exact evaluations of objective function and, on the other hand, provides a fast and reasonably accurate computational feedback in the framework of GAs search.

In this work we use Reduced-Order Models approach in the form of Local Approximation Method (LAM). With the ROM-LAM method, the solution functionals which determine a cost function and aerodynamic constraints (such as pitching moment, lift and drag coefficients), are approximated by a local data base. The data base is obtained by solving the full Navier-Stokes equations in a discrete neighbourhood of a basic point positioned in the search space.

Thus the above mentioned requirements to the computational agent, related to its computational efficiency, are fulfilled. However, an additional effort should be made in order to ensure the accuracy and robustness of the method.

To overcome the approximate nature of the approach, a multidomain prediction-verification principle is employed. That is, on the prediction stage the genetic optimum search is concurrently performed on a number of search domains. As the result each domain produces an optimal point, and the whole set of these points is verified (through full Navier-Stokes computations) on the verification stage of the method, and thus the final optimal point is determined.

Besides, in order to ensure the global character of the search, it is necessary to overcome the local nature of the above approximation. For this purpose it is suggested to perform iterations in such a way that in each iteration, the result of optimization serves as the initial point for the next iteration step (further referred to as optimization step).

COMPUTATIONAL EFFICIENCY

Aerodynamic shape optimization is an example of a highly challenging integral problem. To solve it we need to resolve a number of non-trivial partial problems: 1) to create robust, accurate and efficient full Navier-Stokes solver, 2) to find an appropriate global geometrical representation of optimized shape and 3) to develop an efficient optimal search able to handle various non-linear constraints.

Nevertheless, even a successful solution of all the three partial problems is not sufficient. The point is that the overall computational time needed to obtain the solution is prohibitively high due to significant computational cost of full Navier-Stokes CFD runs and huge number of the runs.

This was partially improved by decreasing the total number of heavy CFD runs in the framework of the ROM-LAM approach. In order to achieve a further decrease of the computational volume, an embedded multilevel parallelization strategy was used: Level 1 - Parallelization of the full Navier-Stokes solver; Level 2 - Parallel CFD scanning of the search space; Level 3 - Parallelization of the GAs optimization process; Level 4 - Parallel optimal search on multiple search domains; Level 5 - Parallel grid generation.

The first two levels are intended to improve the computational efficiency of the CFD component of the whole algorithm, while the next two levels are needed in order to reach the same goal for the optimization part of the method. The fifth parallelization level deals with grid generation.

Multilevel parallelization strategy based on the PVM software package was implemented on a cluster of 216 MIMD multiprocessors.

An additional source of decreasing the volume of computational work is the use of computational grids coarser than those needed for exact estimations of the objective function. It is feasible if the grid coarsening preserves the hierarchy of fitness function values on the search space (that is, the relation of order is invariant with respect to grid coarsening).

Finally, the cumulative effect of the described techniques allowed to reduce the overall time needed for a one-point 2D wing optimization to 5-6 hours on the above cluster. Note, that the direct application of the Genetic Algorithms to the solution of the same problem on a single processor from the cluster, requires about 32 years.

ANALYSIS OF RESULTS

The method was applied to the problem of multipoint transonic 2D and 3D wing optimization with nonlinear constraints. The results include a variety of optimization cases for two classical wings: a 2D test-case of RAE2822 airfoil and a 3D optimization of ONERA M6 wing.

In order to verify the optimization method as a whole, both consistency check as well as

comparison with available results of other authors were performed.

The first test case was to find an optimal 12% thickness 2D airfoil at the design point $C_L = 0.0$, $M = 0.6$ in the fully turbulent flow regime.

The resulting optimal shape should be symmetric, and the verification of this property is a good test to check the consistency of results. To make the problem more challenging, a highly asymmetric supercritical RAE2822 airfoil was chosen as an initial point of the iterative optimization algorithm.

The optimization problem was solved twice, based on CFD computations employing the coarse and medium grids and final results were verified through the fine grid computations. The value of the total drag coefficient C_D was equal equal to 74.1 and 73.5 drag counts, respectively.

The resulting optimal profiles are fairly symmetrical. An additional indication to the symmetry of the optimal solution may be found in fig. 1, where the surface pressure distribution for the airfoil optimized on the medium mesh is given.

To further verify the optimization method, the following multipoint optimization of RAE2822 airfoil was employed. The main design point was $M = 0.734$, $C_L = 0.8$, $Re = 6.5 \cdot 10^6$ (point 1) while the secondary design points were: $M = 0.754$, $C_L = 0.74$, $Re = 6.2 \cdot 10^6$ (point 2) and $M = 0.680$, $C_L = 0.56$, $Re = 5.7 \cdot 10^6$ (point 3). The target was to minimize a weighted combination of total drag values at these points with the following weight coefficients: $w_1 = 0.5$, $w_2 = 0.25$, $w_3 = 0.25$. The constraints were imposed on airfoil thickness and leading edge radius which can not decrease. The comparison of drag reduction achieved by the current optimization tool OPTIMAS with the corresponding AEROSHAPE results [5] is summarized in Table 1.

Table 1: Drag reduction (counts)

Design Point	OPTIMAS	Ref. [4]
1	-59.0	-40.0
2	-103.0	-34.0
3	+2.0	+3.0

It was interesting to check the performance of the method starting from an airfoil which already possesses a fairly good aerodynamic behaviour at the point of design. As the starting point we took a 18% thickness airfoil which was the result of multipoint optimization by means of the commercial code MSES [6] at the following two design points: $M = 0.6$, $C_L = 0.4$ (point A) and $M = 0.4$, $C_L = 0.75$ (point B) . The transition was fixed at 30% of the chord on both upper and lower surfaces.

The current method was applied to the following cases: two single point optimizations (at the above mentioned design points) and a multipoint optimization using a weighted combination of the total drag values at the same points: $C_D = 0.6 \cdot C_D(A) + 0.4 \cdot C_D(B)$.

The results of the optimization are presented in fig. 2-3. In fig. 2, the drag polar at $M = 0.60$ for the original airfoil is compared with those corresponding to the above one- and two-point optimizations, while the aerodynamic shapes at $M = 0.40$ are presented in fig. 3.

It may be observed that also in this case the method (in both a one-point and two-point mode) allowed to obtain a significant improvement of the aerodynamic performance at the design points as well as far beyond them. It is important, that the two-point optimization, compared to the one-point optimizations, results in an airfoil shape which possesses almost identical drag value at point A while the respective value of C_D at point B is only slightly higher.

In the following, we present the results of one- and multi-point drag minimization of ONERA M6 wing at $Re = 11.72 \cdot 10^6$ and different values of design C_L and Mach numbers representing a wide range of flight conditions. A total of 10 test cases was studied. Design conditions and constraints are summarized in Table 2. The corresponding optimal wing shapes are designated by $Case\_1$ to $Case\_10$. In all the optimization cases, the number of wing sections subject to design was equal to N_{ws}.

The optimization at the design point $C_L = 0.265$, $M = 0.84$ ($Case\_1$ - moderate target lift coefficient) resulted in the destruction of a strong double-shock, present in the original

Table 2: Summary of test cases

Case	C_L^*	M	W_i	C_M^*	N_{ws}
1	0.265	0.84	1.0	$-\infty$	2
2	0.500	0.84	1.0	$-\infty$	2
3	0.500	0.86	1.0	$-\infty$	2
4	0.500	0.87	1.0	$-\infty$	2
5	0.500	0.87	1.0	-0.100	2
6	0.500	0.87	1.0	-0.075	2
7	0.500	0.87	0.6	$-\infty$	2
	0.400	0.85	0.4	$-\infty$	2
8	0.500	0.87	1.0	$-\infty$	3
9	0.500	0.87	1.0	-0.100	3
10	0.500	0.87	1.0	-0.100	4

pressure distribution. The optimized wing exhibits a shockless behaviour along the whole wing span which leaded to a significant reduction in the total drag: from 168 drag counts to 128 counts. Note, that the ideal induced drag for the ONERA M6 aspect ratio at $C_L = 0.265$ is equal to 59 counts, and the minimum drag value is equal to about 71 counts for the both wings. Thus it may be concluded that the contribution of wave drag to the total drag of the optimized wing is of a minor nature, which is indicative of successful optimization.

At given free-stream Mach and Reynolds numbers, the off-design performance of a wing can be estimated through the lift-drag polar. The corresponding results are presented in fig.4 where the drag polar for the optimized wing ($Case\_1$) is compared with the original one. It is seen that the optimized wing possesses a significantly lower drag not only pointwise but also for all positive lift values.

Fig.4 also illustrates the convergence of the optimization algorithm. The full convergence was achieved after 7 optimization steps, but already after 5 steps the result was close to the final one. By order of magnitude, such convergence rate is typical of the optimization process for all the test cases considered in this work.

Another important aspect of the off-design performance of wings is their drag rise behaviour at fixed C_L. For $Case\_1$ these data are given in fig.5, where drag polars of the optimized wing for different Mach numbers are shown. It can be assessed that in a wide range of lift values, the drag divergence occurs at least not before $M = 0.87$, which is an essential improvement compared to the original ONERA M6 wing.

Now let us analyze the results of optimization at a much more demanding design point characterized by high target lift coefficient at high free-stream Mach number ($C_L = 0.5$, $M = 0.87$ - $Case\_4$–$Case\_10$).

At these flight conditions, the original ONERA M6 geometry generates a very strong shock which results in a high total drag value (C_D=544 counts). Similar to the previous case the optimization allowed to essentially decrease the total drag down to C_D=300 counts ($Case\_4$). At this point, the theoretical induced drag for the ONERA M6 at $C_L = 0.5$ is equal to 209 counts, while the minimum drag value is equal to about 87 counts for the original wing. In fact, this indicates a very low level of wave drag for the optimized wing.

The influence of the Mach design value (at the same target C_L) on the off-design performance of optimized wings is illustrated in fig.8-9.

In fig.8 lift/drag polars for $Case\_3$ ($M = 0.86$) are compared with the respective curves for $Case\_4$ ($M = 0.87$) at different Mach numbers: $M = 0.84$, $M = 0.87$ and $M = 0.90$. It is seen that the optimized shapes exhibit a consistent behaviour with the results close one to another in the vicinity of the target C_L at the free-stream Mach numbers lower or equal to 0.87.

Drag rise curves of the wings optimized at $C_L = 0.5$ for different design free-stream Mach numbers are compared to that of the ONERA M6 wing in fig.9. It may be concluded that the optimization allowed to significantly shift the drag divergence point in the direction of higher Mach numbers and to radically extend the low drag zone. The shift is greater for a greater design Mach number with a small pay-off for $0.77 \leq M \leq 0.85$.

As mentioned above, in the case of the 3D optimization there exists an additional class of constraints to be taken into account: the aerodynamic constraints such as constraint on the pitching moment C_M. The results of optimization indicate that the present approach is also able to efficiently handle this class of con-

straints. Several optimization cases, with different values of C_M^* (maximum allowed value of the pitching moment) were considered. In fig.10 drag polars at $M = 0.87$ for different C_M^* are shown.

The unconstrained optimum wing ($Case\_4$) possesses $C_M = -0.15$ and $C_D = 300.0$ counts at the design point $M = 0.87$, $C_L = 0.5$. A constrained optimization with $C_M^* = -0.10$ ($Case\_5$) achieved a similar drag reduction ($C_D = 300.5$ counts) while for $C_M^* = -0.075$ ($Case\_6$) the optimized wing possesses a slightly higher $C_D = 305.0$ counts at the same design point. It is important to underline, that up to $C_M^* = -0.10$ the total drag of optimized wings is weakly influenced by C_M^* not only at the design point but also in the off-design zone $C_L > 0.3$.

Thus the following two conclusions may be drawn. First, the performance of unconstrained pitching moment optimization can be sometimes achieved by a constrained optimization even with a rather significant increase in the maximum allowed value of the pitching moment. Second, the same optimal total drag value C_D may be obtained by markedly different aerodynamic shapes. In other words, the considered optimization problem is ill-posed.

On the whole, it may be also assessed that the incorporation of constraints into the optimization problem is twofold. On the one hand, the presence of constraints (as it was explained above) makes the solution of the opimization problem much more complicated. But at the same time, the constrained problem is more well-posed , which facilitates its solution.

Another important issue is the influence of parameter N_{ws} (the number of sectional airfoils) on the optimal solution. This is illustrated in fig. 11 where the comparison of the original M6 root shape with those of wings optimized for different N_{ws}, is given.

The analysis shows that, in the middle part of the wing, the optimal shapes tend to possess low curvature immediately outside the leading edge region. For $N_{ws} = 2$ this leads to a concave form of the above region at the tip section.

Airfoil shapes at the midsection of the optimized wings for $N_{ws} = 3$ and different values of constraint on the wing pitching moment, are shown in fig. 12.

Finally, it is interesting to note that the multipoint optimization allows to improve the wing performance at low C_L with no penalty at the design C_L values.

CONCLUSIONS

A robust hybrid GA/ROM approach to the multipoint constrained optimization of aerodynamic configurations is suggested. Main features of the algorithm include an efficient treatment of nonlinear constraints and scanning of the optimization search space by a combination of full Navier-Stokes computations with the ROM method, along with efficient multilevel parallelization strategy.

The method was applied to the optimization of wings with a variety of nonlinear constraints. The results demonstrated that the method retains high robustness of conventional GAs while keeping CFD computational volume at an acceptable level.

The proposed optimization tool (code OPTIMAS) incorporates state-of-the-art CFD software and innovative optimization algorithms into the core of the aerodynamic design and can be used for practical design of aerodynamic shapes.

REFERENCES

1. B. Epstein, A. Averbuch and I. Yavneh, An accurate ENO driven multigrid method applied to 3D turbulent transonic flows, *J. Comput. Phys.,* **168**, 316 (2001).

2. B. Epstein, T. Rubin and S. Seror, Accurate multiblock Navier-Stokes solver for complex aerodynamic configurations, *AIAA Journal*, **41**, 582 (2003).

3. D. Raveh, Reduced-order models for nonlinear unsteady eerodynamics", *AIAA Journal,* **39**, 1417 (2001).

4. Z. Michalewicz, *Genetic Algorithms + Data Structures = Evolution Programs*, Springer Verlag, New-York, 1996.

5. D. Quagliarella, Airfoil design using Navier-Stokes equations and an asymmetric multi-objective Genetic Algorithm, *Proc. EUROGEN-2003 Conf.,* CIMNE, Barcelona, 2003.

6. M. Drela, Newton solution of coupled viscous/inviscid multielement airfoil flows, *AIAA Paper,* 90-1470, 1990.

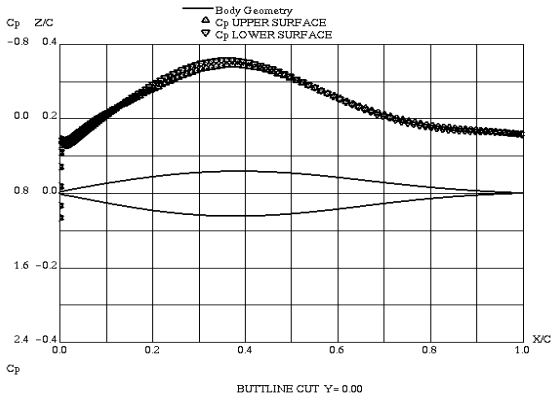

Figure 1: Airfoil optimized on the medium grid at the flight conditions $C_L = 0.0$, $M = 0.6$. Surface pressure distribution at the design point.

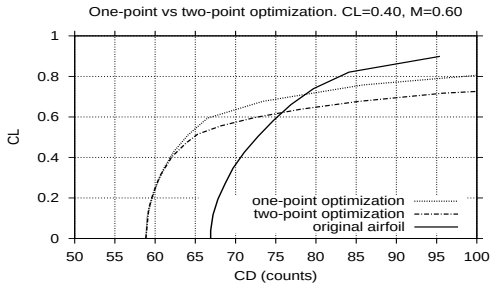

Figure 2: Drag polars at $M = 0.60$. One-point and two-point optimizations vs original airfo

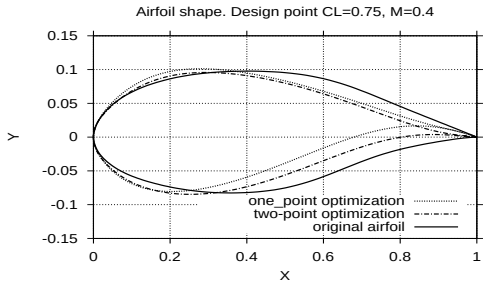

Figure 3: Profile shape. One-point and two-point optimizations vs original airfoil.

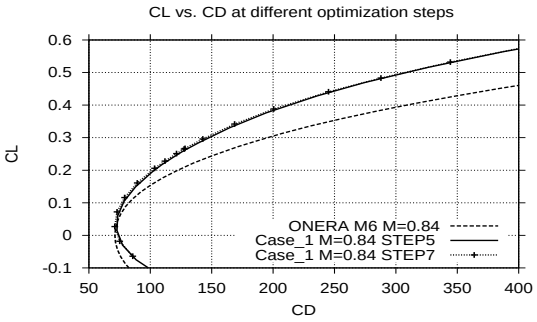

Figure 4: Drag polars at $M = 0.84$. Original ONERA M6 wing vs. optimized wing ($Case\_1$) at different optimization steps.

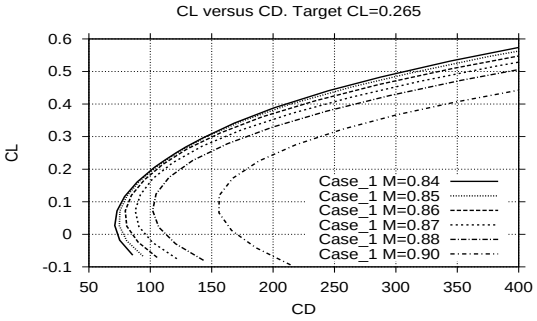

Figure 5: Drag polars of the optimized wing ($Case\_1$) at different free-stream Mach numbers.

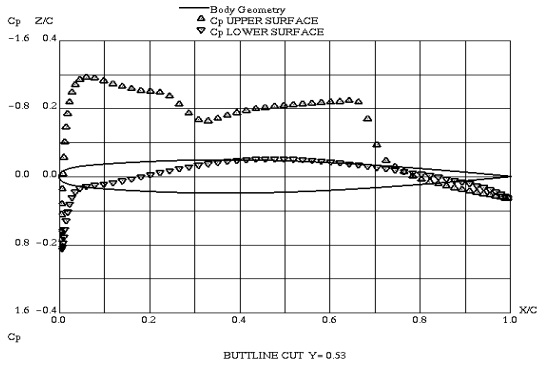

Figure 6: Original ONERA-M6-Wing. Chordwise pressure distribution at the midsection of the wing at M=0.87, $C_L = 0.5$.

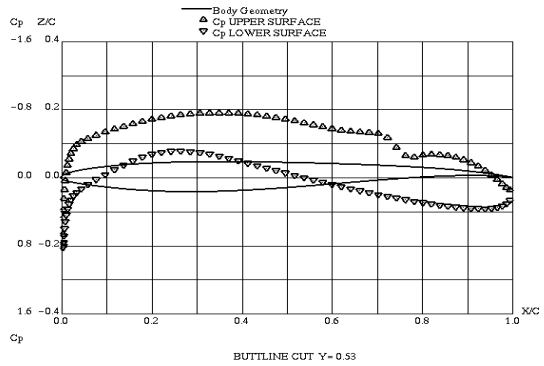

Figure 7: One-point optimization - $Case\_4$. Chordwise pressure distribution at the midsection of the wing at M=0.87, $C_L = 0.5$.

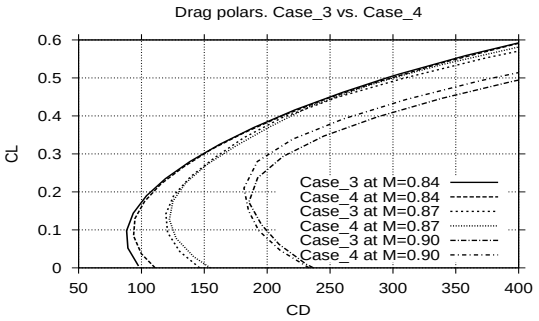

Figure 8: Mach off-design behaviour of optimized wings. Drag polars at different Mach numbers. $Case\_3$ vs. $Case\_4$.

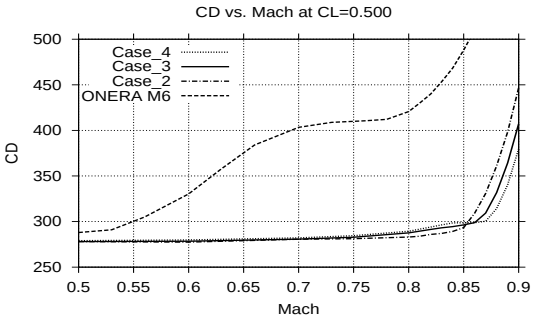

Figure 9: Mach drag divergence of the optimized wings versus the original ONERA M6 wing. $Case\_2$, $Case\_3$ and $Case\_4$ correspond to design M=0.84, 0.86 and 0.87 respectively.

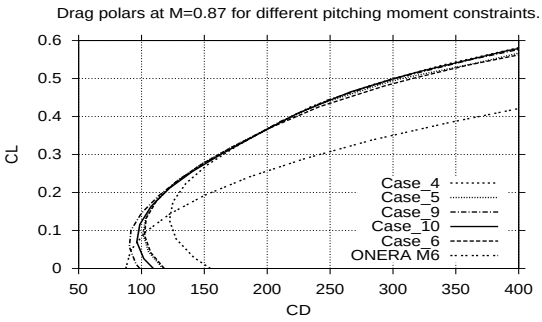

Figure 10: Lift/drag curves at $M = 0.87$. ONERA M6 wing vs. one-point optimizations with different values of constraint on the pitching moment. $Case\_4$: no constraint on C_M; $Case\_5$, $Case\_9$ and $Case\_10$: $C_M \geq -0.1$; $Case\_6$: $C_M \geq -0.075$.

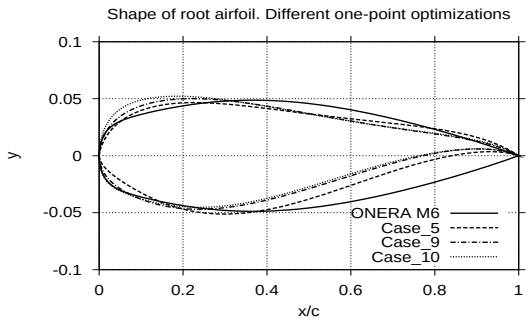

Figure 11: Shape of optimized wings at root section for N_{ws}=2 ($Case\_5$), N_{ws}=3 ($Case\_9$) and N_{ws}=4 ($Case\_10$).

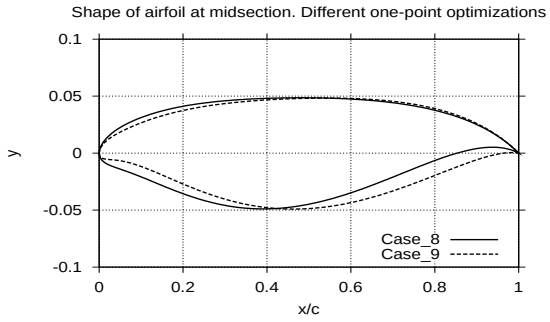

Figure 12: Shape of the optimized wings at midsection for different values of constraint on pitching moment. $Case\_8$ - no constraint on C_M; $Case\_9$ - $C_M > -0.1$. $N_{ws} = 3$.